Dalton Transactions

Accepted Manuscript

ROYAL SOCIETY OF CHEMISTRY

www.rsc.org/dalton

Dalton Transactions

ARTICLE

Received 00th January 20xx,

Accepted 00th January 20xx

DOI: 10.1039/x0xx00000x

www.rsc.org/

Nitrogen-boron coordination versus OH…N hydrogen bonding in pyridoxaboroles – aza analogues of benzoxaboroles

I. Steciuk,[a] K. Durka,[a] K. Gontarczyk,[a] M. Dąbrowski,[a] S. Luliński*[a] and K. Woźniak[b]

Pyridoxaboroles – fused heterocyclic systems composed of pyridine and five-membered oxaborole rings – have been obtained for the first time from simple halopyridines. Thus, 6-butyl-2-(3'-bromo-4'-pyridyl)-(N-B)-1,3,6,2-dioxazaborocan obtained from 3-bromopyridine was converted into a lithio derivative by Br/Li exchange using *n*BuLi/THF at -85 °C. This intermediate was trapped with benzaldehydes to give corresponding pyridoxaboroles after hydrolysis. The use of chlorodiphenylsilane as electrophile gave rise to a related pyridosiloxaborole. The fluorinated pyridoxaborole was obtained by deprotonation of α-(2-methoxyphenyl)-2-fluoro-4-iodopyridylmethanol with NaH and consecutive iodine-lithium exchange/boronation followed by hydrolysis. Single-crystal X-ray analysis of pyridino[4,3-c]-1,3-dihydro-1-hydroxy-3-mezytyl[2,1]oxaborole revealed the formation of a unique 1D coordination polymer based on N–B dative bonds between monomeric molecules. In contrast, the crystal structure of 2-fluoropyridino[4,3-c]-1,3-dihydro-1-hydroxy-3-(2'-methoxyphenyl)[2,1]oxaborole features an infinite H-bonded chain as the main structural motif. The presented considerations are quantified in terms of various computational methods (single molecule and dimer energy calculations, electron density topology, NBO analyses) providing comprehensive picture of structural properties of pyridoxaboroles.

Introduction

Arylboronic acids and their various derivatives (esters, aryltrifluoroborate salts, etc.) constitute a very important class of organic compounds with numerous and diverse applications.[1] In the past few years, there has been a rapidly growing interest in benzoxaboroles (Chart 1, **I**) – a group of boracyclic compounds, which can be described as cyclic hemiesters of 2-(hydroxymethyl)phenylboronic acids.[2] A structural specifity of benzoxaboroles is based on the inclusion of the boron atom into the five-membered ring. As a result, a trigonal planar geometry around the boron atom is significantly distorted as the bond angles differ significantly from the standard value of 120°. Thus, in general benzoxaboroles are stronger Lewis acids than respective arylboronic acids possessing the $B(OH)_2$ functionality.[3] However, the major attention is paid recently to a biological activity of benzoxaboroles.[2,4,5] It was stimulated by the discovery that selected functionalized benzoxaboroles exhibit promising antimicrobial activity. One of these compounds, Tavaborole (AN2690, trade name Kerydin),[6] was approved in July 2014 as a topical antifungal medication for the treatment of onychomycosis - a fungal infection of the nail and nail bed. The discovery of its mechanism of action enabled rational design of other biologically active benzoxaboroles, that are currently under clinical trials.[5] Benzoxaboroles exhibit also sufficient solubility in water at neutral pH and show high affinity and specificity for binding biological relevant diols such glucose, fructose or dopamine, which was extensively exploited for sensing applications.[7] In our latest contribution we showed that similar applicability can be envisioned for benzosiloxaboroles (**II**) – the silicon analogues of benzoxaboroles, where a carbon atom in the oxaborole ring is replaced by a silicon atom.[8]

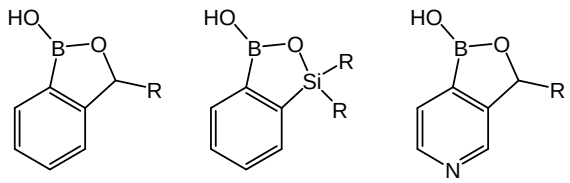

I II III

Chart 1. General structures of benzoxa-, benzosiloxa- and pyridoxaborole.

In general, boronic acids and their derivatives can serve as versatile tectons[9] in crystal engineering and supramolecular chemistry as they are cabable of forming extended hydrogen-bonding networks.[10] They can also produce covalently linked oligomeric or macromolecular aggregates such as boroxines[11] and Covalent Organic Frameworks (COFs).[12] COFs received considerable attention due to their potential applications for gas storage, separation and catalysis. The assembly can be also achieved through dative N–B bonds.[13,14] Moreover, it was demonstrated that

[a] Warsaw University of Technology, Faculty of Chemistry, Physical Chemistry Department, Noakowskiego 3, 00-664 Warsaw, Poland
[b] University of Warsaw, Department of Chemistry, Pasteura 1, 02-093 Warsaw, Poland

† Electronic Supplementary Information (ESI) available: spectroscopic data and titration curves are available for free of charge. CCDC 1406327-1406328. For ESI and crystallographic data in CIF or other electronic format see DOI: 10.1039/x0xx00000x

some arylboronic esters that possess donor and acceptor sites in same molecule (*e. g.,* nitrogen atom and boronate group, respectively) can spontaneously assemble to give polymeric or macrocyclic structures. In contrast, benzoxaboroles have been largely unexplored in fields related to crystal engineering, coordination chemistry and macromolecular chemistry. An exception is the utilization of benzoxaboroles as ligands for 13 group metals.[15] The structural characterization of benzoxaboroles revealed that they usually display simple H-bonded centrosymmetric dimeric motifs in the solid state.[2ad,16]

Herein we report on the synthesis and characterization of pyridoxaboroles (**III**). They can be described as benzoxaboroles congeners in which the benzene ring is replaced with the pyridine heterocycle. Specifically, we were interested how the presence of the nucleophilic nitrogen atom will influence the properties of obtained systems with respect to their benzo counterparts. In this work, we show that pyridoxaboroles can be regarded as building blocks for the construction of supramolecular assemblies based either on the N–B coordination or N…H–O hydrogen bonding. We explain this varying behaviour in terms of different donor properties of the nitrogen atom.

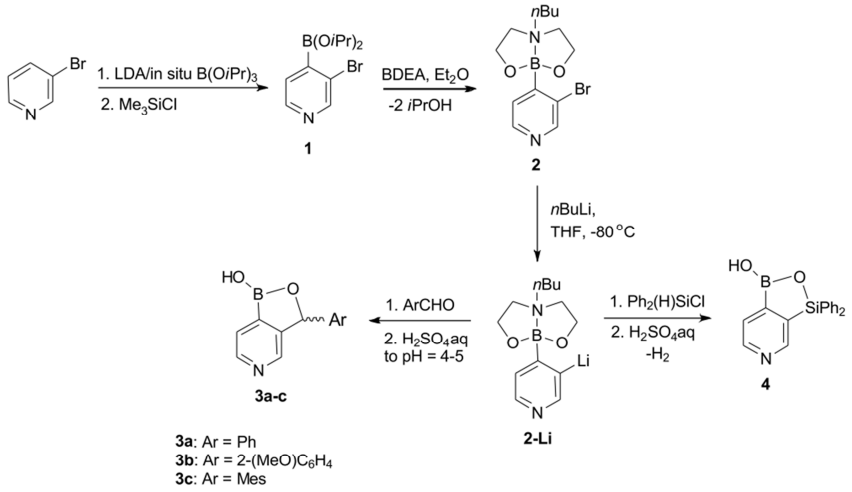

Scheme 1. Synthetic route to pyridoxaboroles **3a-c** and **4**.

Results and discussion

Synthesis

The synthesis of pyridoxaboroles was accomplished using the general approach involving the temporary protection of arylboronic acids with *N*-butyldiethanolamine (BDEA), which leads to the formation of corresponding 6-butyl-2-(aryl)-(*N*-*B*)-1,3,6,2-dioxazaborocans (BDEA esters) featuring the presence of a tetracoordinate boron atom.[17] The method based on the formation of bimetallic lithium-boron intermediates was successfully employed for the synthesis of various functionalized arylboronic acids and esters.[18] Specifically, *ortho*-lithiated phenylboronic BDEA ester was converted into 3-aryl-1-hydroxybenzoxaboroles upon the reaction with selected benzaldehydes followed by hydrolysis of resulting adducts and spontaneous intramolecular dehydrative cyclization.[19] In this work the synthesis started with lithiation/*in situ* boronation[20] of 3-bromopyridine with LDA/B(O*i*Pr)$_3$[20a] followed by the addition of Me_3SiCl, which afforded diisopropyl 3-bromopyridine-4-boronate **1** (**Scheme 1**). It was treated with BDEA in Et_2O to give 6-butyl-2-(3'-bromo-4'-pyridyl)-(*N*-*B*)-1,3,6,2-dioxazaborocan **2**, which precipitates as a white crystalline material from the reaction mixture. It should be preferably isolated under inert atmosphere and stored in cold as it undergoes slow degradation recovering 3-bromopyridine due to a hydrolytic cleavage of a B-C bond upon interaction with moist air at ambient conditions. In the next step, a solution of **2** in THF was added to a solution of *n*BuLi in THF at –85 °C which afforded a yellow suspension of a desired bimetallic boron-lithium reagent **2-Li**. Treatment of **2-Li** with selected benzaldehydes (PhCHO, (2-MeO)C_6H_4CHO, MesCHO) and hydrolysis with aqueous H_2SO_4 afforded corresponding pyridoxaboroles **3a-c** in good yields (81%-98%). To avoid the protonation of the nitrogen atom the final pH of the mixture should range from 4-5. In addition we have attempted to obtain a pyridoxaborole analogue possessing the silicon atom in the oxaborole ring, *i.e.*, replacing the C3 carbon atom in the oxaborole ring. Thus, following our recently published protocol,[8] **2-Li** was trapped with Ph_2(H)SiCl and subsequent hydrolysis (final pH = 4) accompanied by evolution of dihydrogen gave the product **4** which precipitated immediately from the reaction mixture. Unfortunately, **4** is essentially insoluble in common solvents. It is only sparingly soluble in DMSO-d_6 acidified with a drop of TfOD, Presumably, a respective pyridinium derivative is generated under these conditions. The ^{1}H NMR spectrum shows broadened signals of pyridine H atoms, which indicates that the resulting species undergoes some some dynamic processes in DMSO-d_6 solution.

We have elaborated another synthetic strategy leading to pyridoxaborole **5b** (**Scheme 2**). Thus, 2-fluoropyridine was converted into 2-fluoro-3-iodopyridine.[21] Then, the treatment with LDA at –78 °C gave the 4-lithio derivative which underwent immediately basicity-gradient driven isomerization to give more stable 2-fluoro-3-lithio-4-iodopyridine.[22] It was trapped with 2-methoxybenzaldehyde to afford α-(2'-methoxyphenyl)-2-fluoro-4-iodopyridine-3-methanol **5a**. It was protected in the form of a sodium salt using NaH and then treated with *t*BuLi. The lithiate was reacted with B(OMe)$_3$ and the resulting adduct was hydrolyzed to give **5b**. Compounds **3a-c** are white solids soluble in MeOH and DMSO but in contrast to related benzoxaboroles they are insoluble in other common solvents including THF, acetone and acetonitrile. The fluoro derivative **5b** is well soluble in all aforementioned solvents. All obtained products are stable in the solid state at ambient conditions. They also exhibit reasonable stability in solution since the respective NMR spectra confirming the targeted structures were unchanged at least for several days. Specifically, ^{1}H and ^{13}C NMR spectra of **3c** indicate that the rotation of the mesityl group is hampered, which is manifested by the presence of separate broadened ^{1}H NMR resonances of two *ortho*-Me groups at

2.49 and 1.56 ppm. Accordingly, there are also two broadened resonances of aromatic protons at 6.91 and 6.65 ppm. The similar behavior was previously observed for related benzoxaboroles.[19] We have also attempted to study the solution behaviour of pyridoxaboroles by the ^{11}B NMR spectroscopy. The ^{11}B NMR spectra of **3a-c** and **5b** in DMSO-d_6 show the broad signals in the range of 32-34 ppm which means that these compounds exists under these conditions as monomeric molecules in a classical form featuring a three-coordinate boron atom. In contrast, in MeOH/D_2O the ^{11}B NMR resonance of **3b** is shifted to 9 ppm, which indicates the quaternization of the boron centre. In the case of **5b**, the ^{11}B NMR chemical shift in this mixed protic solvent is ca. 27.5 ppm, i.e., it is lower by ca. 5 ppm than the value found for a DMSO solution. We suppose that under these conditions **3b** forms a zwitterionic species bearing the protonated nitrogen atom and the anionic boronate moiety upon reaction with water or methanol (**Fig 1**). Such a behavior was previously observed for simple pyridineboronic acids.[23] It may also be the case for **5b**, but the protonation of nitrogen atom seems to be difficult due to its much lower basicity resulting from the strong electron-withdrawing effect of 2-fluoro substituent. This is supported by the comparison of pK_{aH} values for pyridine (5.17) and 2-fluoropyridine (–0.44).[24] Thus, a slightly decreased δ^{11}B value may simply reflect a rapid equilibrium between the classical neutral form of **5b** and the respective boronate anion. We observed a similar effect for some fluorinated 1,2-phenylenediboronic acids.[25] This equilibrium is shifted of course to the side of the former species at weakly acidic pH produced upon dissolving **5b** in MeOH/D_2O.

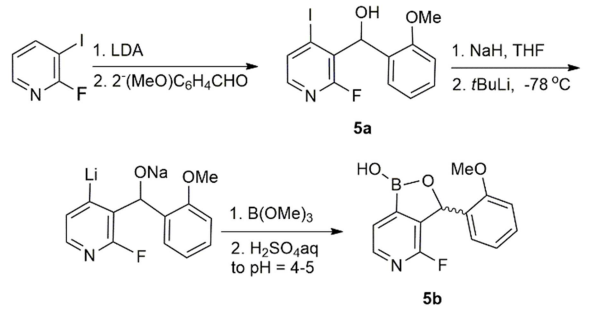

Scheme 2. Synthetic route to pyridoxaborole **5b**.

The specifity of pyridoxaboroles relies on the presence of a Lewis basic nitrogen atom which opens a possibility for further reactions involving interactions with electrophilic reagents. These include the protonation performed by addition of HCl to compound **2b** and methylation effected by refluxing the suspension of **2b** with Me_2SO_4 in acetonitrile (**Scheme 3**). Unlike the starting material, the

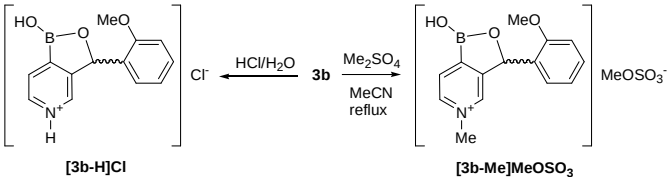

Scheme 3. Synthesis of pyridinium derivatives of **3b**.

obtained pyridinium salts **[3b-H]Cl** and [**3b-Me**][**MeOSO$_3$**] are well soluble in water, which may be important from the point of view of biological applications.

Acidity of pyridoxaboroles

In order to evaluate the acidity of pyridoxaboroles we have subjected compounds **3b-c, 5b** to a potentiometric titration with 0.1 M aqueous NaOH in H_2O/MeOH (1/1). The pK_a values were estimated to be in the range of 7.2-7.6 for **3a-c**. For comparison, we have found (under the same conditions) that the pK_a of the benzo analogue of **3b**[19] was 7.4. Overall, these values are comparable to that reported for simple benzoxaborole where pK_a = 7.3.[3] All studied compounds are significantly stronger acids than phenylboronic acid and its many functionalized derivatives, where typical pK_a values are about 9.[26] This was explained in terms of the increased strain around the trigonal planar boron atom in the five-membered oxaborole ring which is released upon acceptance of hydroxide anion.[3] However, taking into account the results of ^{11}B NMR spectroscopy studies, the acid-base equilibrium in pyridoxaboroles can be alternatively described as the dissociation of the NH$^+$ group. Furthermore, the pK_{a1} of **[3b-H]Cl** was determined to be 3.5 which is lower than the value obtained for a related 3-boronated pyridinium cation, where the pK_{a1} = 4.0 was reported.[23] Thus, pyridoxaboroles can exist in different forms in aqueous solution depending on the pH, which is due to their amphoteric nature. For instance, **3b** is stabilized as the zwitterion in the pH range of 3.5-7.4, whereas the corresponding pyridinium cation and boronate anion persist at lower and higher pH, respectively (**Fig 1**). Compound **5b** features a much lower pK_a of 5.2, which might be explained by a strong acidifying effect of fluorine on the adjacent NH$^+$ group.[27] However, as already mentioned, in this case it seems rather unlikely that the N atom is protonated[23] unless strongly acidic conditions are involved.

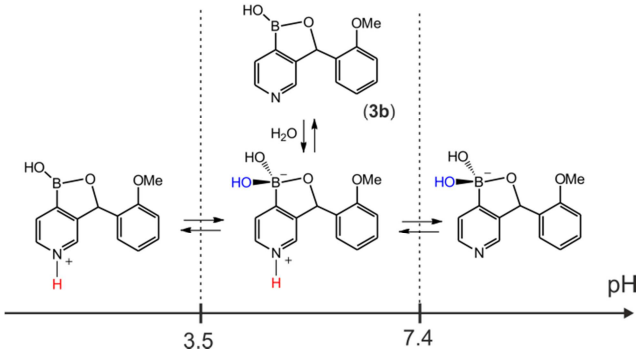

Figure 1. Various forms of **3b** in aqueous solutions.

Thermal behaviour

The DSC-TGA analysis of studied pyridoxaboroles show a quite different thermal behavior of these compounds due to different structural properties. The DSC-TGA curves of pyridoxaboroles **3c** (as a representative compound for a series **3a-c**), **4** and **5b** are given in **Fig 1**, individual DSC and TGA curves of all studied compound are given in ESI. The structures of studied compounds are stable up to ca. 140 °C. Further heating leads to a solid-liquid phase transition.

However, according to visual observations and DSC measurements, **3a-c** melt in a wide temperature range. On the other hand, **5b** melts sharply (174–176 °C). The TGA analyses show that these processes are accompanied by releasing one mole of water per two equivalents of pyridoxaborole. This is consistent with the formation of dimeric anhydrides (diboroxanes) featuring B–O–B moiety (**Scheme 4**). In the case of **5b** this was also confirmed by ^{1}H NMR as a spectrum of a sample heated at 150 °C in vacuo for 1 hr was similar to that recorded for the original one but it showed only residual resonance of the BOH proton. In the case of **3a**, dehydration seems to occur below the melting point determined by DSC. At higher temperatures (200–290 °C) **3a-c** and **5b** undergo distinct exothermic processes, which are, however, not accompanied by a significant mass loss. This may be interpreted by a thermal rearrangement whose nature is not clear yet. According to DSC measurement this transition is irreversible as the crystallization is not observed during cooling from 300 °C (see ESI). Furthermore, there are no distinct changes on DSC curve in the reheating cycle. TGA analyses show that the samples lose a significant amount of mass only above 270 °C (**3a-c**) or 340 °C (**5b**). A different thermal behavior is manifested by pyridosiloxaborole **4**. The DSC curve of **4** does not show any distinct changes corresponding to consecutive phase transition, dehydration or rearrangement processes. It loses weight gradually (*ca*. 10%) when heated to 300 °C.

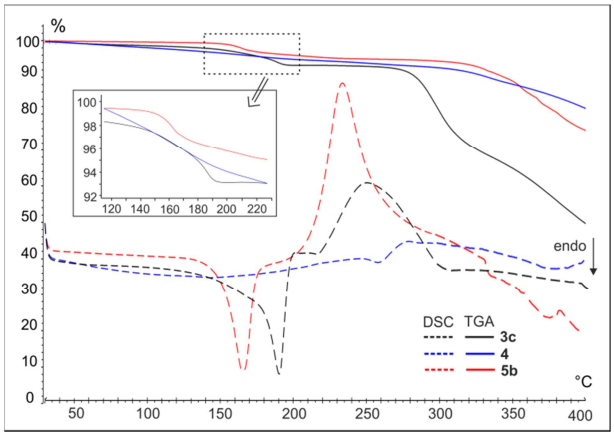

Figure 2. TGA and DSC curves of pyridoxaboroles **3c**, **4** and **5b**.

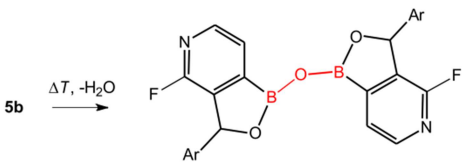

Scheme 4. Thermal dehydration of **5b**.

Crystal structures of 3c and 5b

We were succeeded in obtaining single crystals of **3c** by slow cooling of its solution in warm DMSO. In the case of **5b**, slow evaporation of its solution in acetone at room temperature was effective. Crystal structures of compounds **3c** and **5b** represent two different types of molecular and supramolecular organization. Views of the molecular structures together with the atom labeling scheme are included in **Fig 3**. The X-ray diffraction structural analysis of **3c** revealed that it assembles through dative N–B bonds to a *zig-zag* type coordination polymer chain (**Fig 4a**) running parallel to the [010] crystallographic direction. The neighbouring molecules in a strand have opposite configurations (*i.e.*, *R* and *S*). The dihedral angle between least-square planes of pyridine rings of adjacent monomeric units is close to 110°. The B…B distance between two closest molecules in the chain is 6.052(3) Å and between every second molecule - 10.000(3) Å, which equals to the length of the edge *b* of a unit cell. Due to the formation of N–B dative bond, each boron centre is tetracoordinate with the tetrahedral character (THC)[28] close to 100%. The length of this bond is 1.678(3) Å, which lies within bond distance distribution of other N–B adducts found in Cambridge Structural Database (1.58÷1.72 Å).[29] The OH group is arranged in the O(2)–H(2)…O(1)$^{(2+x, -y, 1-z)}$

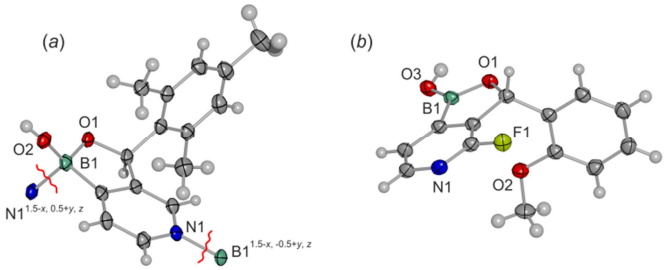

Figure 3. Molecular structure of (*a*) **3c**, (*b*) **5b**. Thermal ellipsoids were generated at the 50% level of probability. Selected bond distances (Å) and angles (deg) for **3c**: C3–B1 = 1.576 (1), B1–O1 = 1.379(1), B1–O3 = 1.337(1), C3–B1–O1 = 108.1(1), C3–B1–O3 = 127.7(1), C1–C2–C6–C7 = 87.5(2). Selected bond distances (Å) and angles (deg) for **5b**: B1–N1$^{(1.5-x, 0.5+y, z)}$ = 1.678(3), B1–O1 = 1.477(3), B1–O2 = 1.403(3), C15–B1 = 1.626(3), C15–B1–O1 = 101.9(2), C15–B1–N1$^{(1.5-x, 0.5+y, z)}$ = 108.4(2), C13–C14–C4–C3 = 93.3(2).

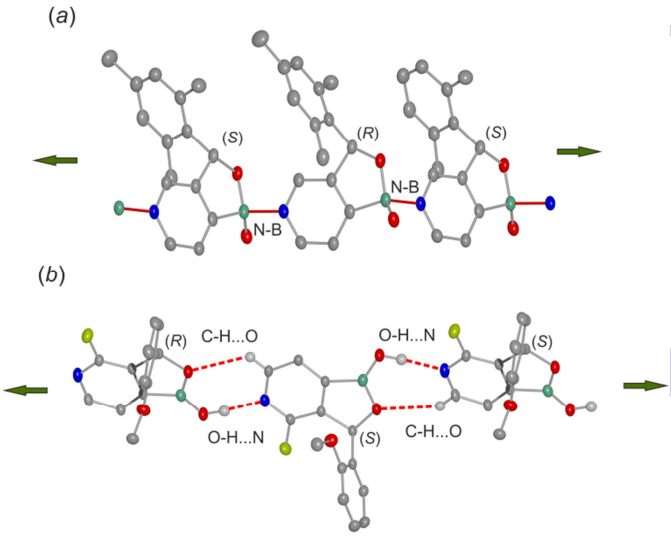

Figure 4. (a) N–B coordination polymer in **3c**, (b) hydrogen bonded chain in **5b**. The dative N–B bonds and the hydrogen bonds are marked as red solid and red dashed lines, respectively.

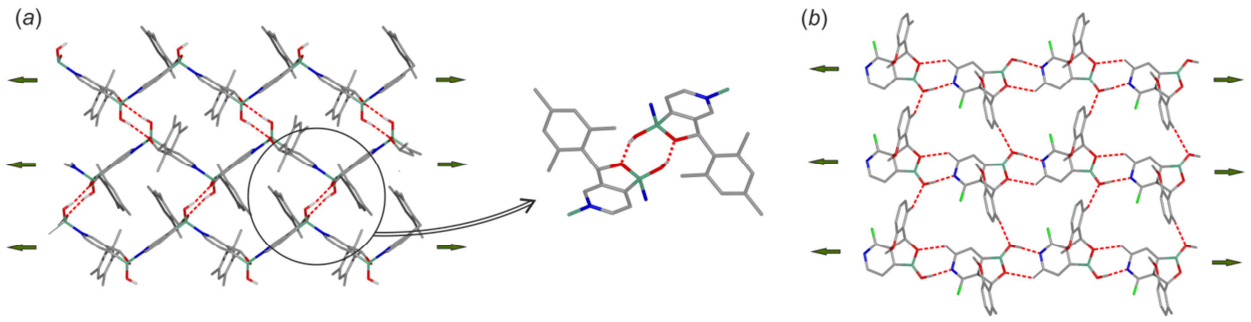

Figure 5. Crystal structure stereoviews showing the aggregation of polymeric chains (**3c**) and hydrogen-bonded chains (**5b**) via secondary O-H…O (**3c**) and C-H…O (**5b**) hydrogen-bond interactions.

intermolecular hydrogen bond ($d_{O...O}$ = 2.823(2) Å, $d_{H...O}$ = 2.008(2) Å) linking molecules **3c** from neighbouring chains. The resulting hydrogen-bonded dimeric motifs resemble those typical of benzoxaboroles.[16] Due to these interactions the 1D coordination polymer chains are organized into (001) layers (**Fig 5a**).

Structurally related boron supramolecular systems have been previously obtained by Severin[13] and Höpfl.[14] They showed that 3- and 4-pyridineboronic as well as 5-isoquinolineboronic esters can serve as self-complementary tectons for the generation of macrocyclic or 1D polymeric boron complexes. It is noticeable that the related pyridineboronic acids form only hydrogen-bonded (O–H…N and O–H…O) networks where the N–B coordination does not occur at all.[30] One could expect a similar structural behaviour for pyridoxaboroles. However, in this case the boron atom exhibits a higher Lewis acidity, which enables its interaction with the pyridine nitrogen atom.

A completely different picture of structural assembly is observed for **5b**. The molecular geometry of this compound is typical of benzoxaboroles with a planar, three-coordinate boron atom (**Fig 3a**).[16] The nitrogen atom is arranged in O(3)–H(3A)…N(1)$^{(0.5+x,\ 0.5-y,\ 0.5+z)}$ interaction ($d_{O...N}$ = 2.742(1) Å, $d_{H...O}$ = 1.82 Å) with the B–OH group. An auxiliary C(5)$^{(0.5+x,\ 0.5-y,\ 0.5+z)}$–H(5)$^{(0.5+x,\ 0.5-y,\ 0.5+z)}$…O(1) contact ($d_{C...O}$ = 3.288(1) Å, $d_{H...O}$ = 2.60 Å) occurs between pyridine moiety and borole oxygen atom. Due to these hydrogen bonds the [101] chain is formed. It comprises molecules featuring opposite configurations in the *RSRS* sequence (**Fig 4b**). The further aggregation of chains occurs via secondary C–H…N and C–H…O interactions (**Fig 5b**). Since it was expected that the boron Lewis acidity in both studied pyridoxaboroles (i.e., **3c** and **5b**) is comparable (or even should be slightly higher for **5b** due to the electron-withdrawing effect of fluorine), the question arose, why **5b** does not self-assemble to form a coordination polymer as observed for **3c**.

Aggregation of pyridoxaboroles – a computational approach

In order to investigate the origin of observed structural diversity of pyridoxaboroles we have performed a series of theoretical calculations using M06-2X[31] functional with 6-31+G(d)[32] basis set. Our intention was to compare the aggregation through O–H…N hydrogen bonds and N–B dative bonds. To simplify the calculations and to get a direct comparison we have studied structures **3c'** and **5b'**, *i.e.*, close analogues of **3c** and **5b** – both bearing phenyl group at C3. At first, we compared the energies of isolated hydrogen-bond and coordination dimers of **3c'** and **5b'** with the geometries taken from corresponding crystal structures **3c** and **5b**, then modified and subjected to optimization. The results are given in **Table 1** and **Fig 6**. The computations revealed that O–H…N dimer interaction energies (ΔE_1) are comparable and equal to –46.3 kJ·mol^{-1} and –41.1 kJ·mol^{-1} for **3c'** and **5b'**, respectively. A more detailed information on the bonding situation within discussed dimers can be derived from topological analyses of electron densities in the framework of QTAIM approach.[33] According to the Espinosa-Lecomte estimation,[34] interaction with energies estimated to be –12.6 kJ·mol^{-1} in both the energies of O–H…N bonds are

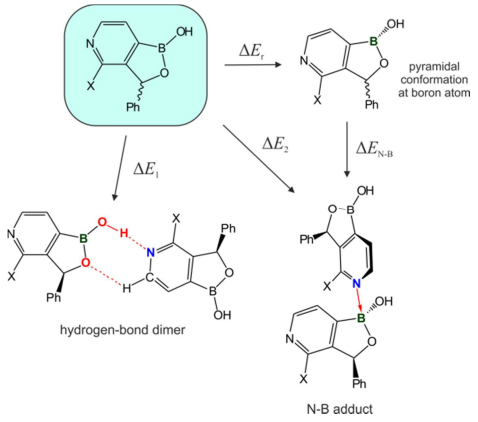

Figure 6. Formation of H-bonded and N–B coordination dimers.

Table 1. The results of quantum-chemical calculations for **3c'** and **5b'**. ΔE_1 – energy of the O–H…N hydrogen bond dimer, ΔE_2 – energy of the N–B coordination dimer, ΔE_{N-B} – energy of the N–B bond, ΔE_r – energy required for the rearrangement from a planar to a pyramidal conformation.

	3c'	**5b'**
ΔE_1 / kJ·mol^{-1}	–46.3	–41.1
ΔE_r / kJ·mol^{-1}	+106.1	+101.7
ΔE_{N-B} / kJ·mol^{-1}	–151.1	–102.4
$\Delta E_2 = \Delta E_r + \Delta E_{N-B}$ / kJ·mol^{-1}	–45.1	–0.6

–34.1 kJ·mol^{-1} (**3c'**) and –30.4 kJ·mol^{-1} (**5b'**). They are supported by the auxiliary C–H…O cases. The sum of O–H…O and C–H…O energy values quite well reproduces the dimer interaction energy derived from the supermolecular method.

The formation of N–B adduct requires rehybridization of a boron centre resulting in its pyramidalization. The energy of this process (ΔE_r) is similar in both molecules and equals to ca. +100 kJ·mol^{-1}. On the other hand, the energy of N–B bond (ΔE_{N-B}) in **5b'** adduct is significantly lower (–102.4 kJ·mol^{-1}) than that in **3c'** (–151.1 kJ·mol^{-1}) and barely counterbalances the rehybridization penalty (ΔE_2 = –0.6 kJ·mol^{-1}). Moreover, the calculations revealed that the **5b'** coordination dimer is unstable and decomposes to give two separate molecules when the N–B bond is not constrained. The further optimization leads to the previously discussed H-bonded dimer. A low stability of the N–B adduct for **5b'** can be rationalized by the lower nitrogen atom Lewis basicity when compared to **3c'** due to a strong electron withdrawing effect of fluorine atom. Moreover, the fluorine substituent increases a steric hindrance in the vicinity of the nitrogen atom and also introduces a repulsive F…O contact in the N–B adduct (the estimated energy of this interaction is ca. +5 kJ·mol^{-1}). A different situation occurs in **3c'** as the energy of the formation of N–B adduct (ΔE_2 = –45.1 kJ·mol^{-1}) is comparable to H-bonded dimer interaction energy.

The nucleophilicity of **3c'** and **5b'** can also be compared in the framework of AIM and Natural Bond Orbital (NBO) population analysis.[35] For these computations, the pyridine molecule was taken as a referential system. The analysis of the negative Laplacian ($L(\mathbf{r}) = -\nabla^2\rho(\mathbf{r})$) function around the nitrogen atoms provides the (3, -3) critical point (CP) corresponding to a local maximum of electron density (CC), which can be associated with the nitrogen lone pair (**Fig 7**). According to expectations, **3c'** shows very similar values of electron density ($\rho(\boldsymbol{r}_{CC})$) and the negative Laplacian in CC_N as pyridine does (**Table 2**). In turn, in **5b'** these values are noticeably smaller. Furthermore, the nucleophilic power of CC sites of a nitrogen atom, which is defined as $L(\mathbf{r}_{CC})/\rho(\mathbf{r}_{CC})$,[36] is higher for **3c'**, which indicates that the nucleophilicity of this compound is more pronounced with respect to **5b'**. Similar conclusions are derived from NBO population analyses. The occupancy of a nitrogen lone pair (N(LP)) is higher in **3c'** (and in pyridine) than in **5b'** (**Table 3**). It is also expected that **3c'** is more reactive based on the comparison of HOMO energies (–0.344 *e*V in **3c'** *vs.* –0.356 *e*V in **5b'**).

The formation of the N–B bonds in a coordination dimers of **3c'** and **5b'** are accompanied by the appearance of a bond paths and a bond critical points (BCP) located close to the boron atoms. The values of $\rho(\boldsymbol{r}_{BCP})$ for these bonds are moderate ($\rho(\boldsymbol{r}_{BCP})$ = 0.72 *e*·A^{-3} for **3c'** and $\rho(\boldsymbol{r}_{BCP})$ = 0.64 *e*·A^{-3} for **5b'**) with the values of the negative Laplacian of –5.6 *e*·A^{-5} (**3c'**) and –5.9 *e*·A^{-5} (**5b'**), which is consistent with the results obtained for (*N-B*)-dioxaazaborocans and other related N–B adducts.[37] As a result of the dative bond formation the charge concentration around the nitrogen atom is significantly reduced (AIM: $\rho(\boldsymbol{r}_{CC})$ = 4.05 *e*·A^{-3} → 3.79 *e*·A^{-3} in **3c'** and 3.96 *e*·A^{-3} → 3.79 *e*·A^{-3} in **5b'**) and the occupancy of the nitrogen lone pair is decreased accordingly (NBO: N(LP) = 1.921 *e* → 1.667 *e* in **3c'** and 1.894 *e* → 1.657 *e* in **5b'**). The formation of the O–H…N hydrogen bond also leads to decreasing electron density in a nitrogen lone pair region but it occurs to a lesser extent (AIM: $\rho(\boldsymbol{r}_{CC})$ = 4.05 *e*·A^{-3} → 3.96 *e*·A^{-3} in **3c'**, 3.96 *e*·A^{-3} → 3.90 *e*·A^{-3} in **5b'**, NBO: N(LP) = 1.921 *e* → 1.884 *e* in **3c'**, 1.894 *e* → 1.859 *e* in **5b'**). The calculated values of electron density and negative Laplacian suggest moderately strong O–H…N intermolecular interactions in **3c'** and **5b'**. It is noticeable that the amount of electron density in the BCP of N–B bond in **5b'** adduct is slightly lower than in **3c'** indicating that N–B interaction in the former compound is weaker.

It should be stressed that in the solid state the large energetic contribution of crystal lattice energy may play a crucial role for the composition and structure of the final form of the compound. Even if monomeric forms of boronic compounds dominate in solution, they might finally crystallize as polymers.

Table 2. Properties of electron density topology around nitrogen atom in pyridine, **3c'**, **5b'** and corresponding dimers.

	CP type	$\rho(\boldsymbol{r}_{CP})$ / e·A^{-3}	$L(\boldsymbol{r}_{CP})$ / e·A^{-5}	$(L(\boldsymbol{r}_{CP})/\rho(\boldsymbol{r}_{CP}))$ / A^{-2}
Pyridine	CC_N	4.04	80.0	19.8
3c' (single molecule)	CC_N	4.05	80.5	19.9
5b' (single molecule)	CC_N	3.96	76.3	19.2
3c' (N-B adduct)	CC_N	3.79	69.2	18.2
	BCP_{N-B}	0.72	-5.6	-
5b' (N-B adduct)	CC_N	3.79	68.5	18.1
	BCP_{N-B}	0.64	-5.9	-
3c' (O-H…N dimer)	CC_N	3.96	76.7	19.4
	$BCP_{O-H...N}$	0.31	-3.0	-
	$BCP_{C-H...O}$	0.06	-0.8	-
5b' (O-H…N dimer)	CC_N	3.90	73.7	18.9
	$BCP_{O-H...N}$	0.30	-3.1	-
	$BCP_{C-H...O}$	0.06	-0.8	-

Table 3. Summary of NBO analyses for nitrogen lone pair orbital in pyridine, **3c'**, **5b'** and corresponding dimers.

		Occupancy / *e*	Hybridi-zation	Orbital energy / *e*V
Pyridine	N(LP)	1.919	$sp^{2.64}$	-0.262
3c' (single molecule)	N(LP)	1.921	$sp^{2.50}$	-0.344
5b' (single molecule)	N(LP)	1.894	$sp^{2.43}$	-0.356
3c' (N-B adduct)[a]	N(LP)	1.922	$sp^{2.43}$	-0.327
	N|→B	1.667	$sp^{3.19}$	-0.392
5b' (N-B adduct)[a]	N(LP)	1.894	$sp^{2.39}$	-0.341
	N|→B	1.657	$sp^{3.03}$	-0.413
3c' (O-H…N dimer)[a]	N(LP)	1.923	$sp^{2.44}$	-0.339
	N|…HO	1.884	$sp^{2.59}$	-0.371
5b' (O-H…N dimer)[a]	N(LP)	1.895	$sp^{2.43}$	-0.351
	N|…HO	1.859	$sp^{2.54}$	-0.388

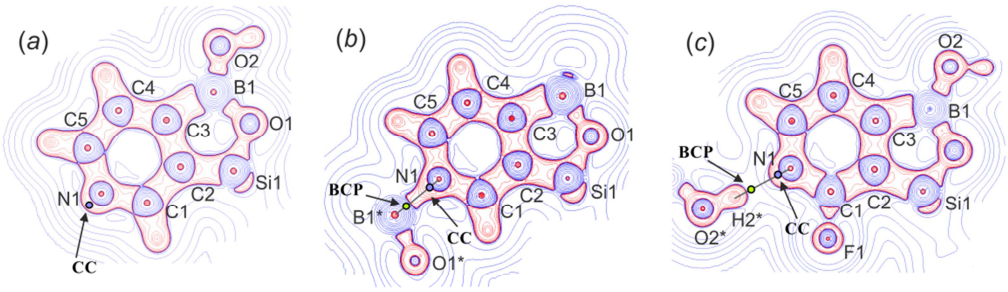

Figure 7. Negative Laplacian ($L(\boldsymbol{r}) = -\nabla^2 \rho(\boldsymbol{r})$) map in the pyridine ring plane for (a) **3c'**, (b) **3c'** N–B adduct and (c) **5b'** O-H…N dimer. Contours are in logarithmic scale ($e \cdot Å^{-5}$), blue solid lines denote positive values and red dashed lines to the negative ones.

Conclusions

In conclusion, synthetic approaches to a novel class of heterocyclic systems composed of fused pyridine and oxaborole rings were developed. Unlike structurally related benzoxaboroles, pyridoxaboroles are amphoteric compounds due to the presence of a basic nitrogen atom. ^{11}B NMR spectroscopic studies point to the formation of zwitterionic species featuring the protonated nitrogen atom and anionic boronate moiety in a mixed MeOH/D_2O solvent. Thus, the acid-base equilibrium seems to be due to the proton abstraction from the NH^+ group. However, the pK_a values for pyridoxaboroles **3a-c** and their benzo counterparts are roughly equal. On the other hand, the effect of fluorination on the acidity seems to be stronger for pyridoxaboroles than for benzoxaboroles. The presence of the Lewis acidic B atom and Lewis basic N atom may also result in a strong tendency to intermolecular interactions by means of N–B dative bonds. Thus, in a solid state, a self-aggregation of **3c** leads to the formation of a 1D coordination polymer. However, the introduction of a 2-fluoro substituent to the pyridine ring destabilizes N–B coordination and leads to the formation of hydrogen-bonded chains as a basic supramolecular motif in the crystal lattice. It is supposed that the structures of remaining (non-fluorinated) pyridoxaboroles presumably resemble the crystal motifs of **3c** rather than those found in **5b** as suggested by their low solubility in common organic solvents.

Comprehensive computational analyses show that N–B coordination dimer of **5b** is rather unstable, while in case of **3c** different forms (*e. g.* single molecule and N–B adducts) may be observed. More detailed analyses show that the topologies of electron density around the nitrogen atom in **3c'** and pyridine are comparable. In the case of **5b'** the values of electron density and nucleophilicity power are lower, which rationalizes a lower tendency of this compound to form N–B adducts. It is also noticeable that the aggregation through N–B coordinate bond does not lead to an increased thermal stability.

Our results demonstrate that pyridoxaboroles can serve as self-complementary tectons for generation of molecular networks through N–B coordination and/or hydrogen bonds. Moreover, the simple variation of substituents may significantly affect the topology of the system and discriminate between the formations of H-bonded networks or N–B aggregates. The specific behaviour of pyridoxaborole results from their amphoteric character, higher boron Lewis acidity as compared to pyridineboronic acids (or esters) and the presence of two competitive electron deficient sites for the interaction with a basic nitrogen atom (the boron and OH hydrogen atom). Further work will be devoted to the synthesis of other pyridoxaboroles and related systems, which will be employed as building units in self-assembly networks. In addition, we are planning to work on further characterization of these compounds. Specifically, this will include studies on their biological activity which hopefully could give rise to applications in medicinal chemistry.

Experimental

General comments.

Solvents used for reactions were dried by heating to reflux with sodium/benzophenone and distilled under argon. Starting materials including 3-bromopyridine, triisopropyl borate, *n*BuLi (10 M solution in hexanes), BDEA, benzaldehydes, chlorodiphenylsilane were used as received without further purification. In the ^{13}C NMR spectra the resonances of boron-bound carbon atoms were not observed in most cases as a result of their broadening by partially relaxed B–C couplings. ^{1}H and ^{13}C NMR chemical shifts are given relative to TMS using residual solvent resonances. ^{11}B and ^{19}F NMR chemical shifts are given relative to $BF_3 \cdot Et_2O$ and $CFCl_3$, respectively. Results of elemental analyses for pyridinium salts **[3b-H]Cl** and **[3b-Me][MeOSO$_3$]** did not match to the given formulae, presumably due to the presence of water or other trace impurities in analyzed samples.

Synthesis.

6-Butyl-2-(3'-bromo-4'-pyridyl)-(N-B)-1,3,6,2-dioxazaborocan (2). A solution of LDA freshly prepared from diisopropylamine (42 g, 58.7 mL, 0.42 mol) and *n*BuLi (10 M; 40 mL, 0.4 mol) in Et_2O (200 mL) was added dropwise to a solution of 3-bromopyridine (63.2 g, 0.4 mol) in THF (250 mL) containing B(O-*i*Pr)$_3$ (82.7 g, 101.5 mL, 0.44 mol) at – 90 °C. The resulting brown slurry was stirred for 20 min at –85 °C, then it was warm to –10 °C, and Me_3SiCl (62 mL, 0.5 mol) was added. Then the reaction mixture was warmed to 40 °C and precipitation of lithium chloride was observed. The mixture was stirred for 30 min, and after cooling to room temperature, the resulting slurry was filtered under an argon atmosphere. The solid was washed with Et_2O (50 mL) and the filtrate was concentrated to

gave a brown oily residue, which was subjected to fractional vacuum distillation to give diisopropyl (3-bromopyridin-4-yl)boronate **1** (b.p. 88-92 °C / 1 Tr) as a yellowish oil, which forms a solid on cooling. Yield 88.7 g (78%). A solution of *N*-butyldiethanolamine (40.2 g, 0.25 mol) in Et_2O (50 mL) was added dropwise to a solution of **1** (70.0 g, 0.25 mol) in Et_2O (200 mL) at 5 °C. The temperature was kept below 10 °C during the addition. The precipitation of a white crystalline material was observed. Stirring was continued for 30 min, and then the resulting solid was filtered and washed with cold Et_2O (2 × 50 mL). Drying in vacuo gave the title compound (75 g, 92%), m.p. 112-114 °C. ^{1}H NMR ($CDCl_3$, 400 MHz) δ = 8.60 (s, 1H, Py), 8.38 (d, J = 4 Hz, 1H, Py), 7.65 (d, J = 4 Hz, 1H, Py), 4.15 (m, 4 H, CH_2O), 3.30 (m, 2H, CH_2N) 3.09 (m, 2H, CH_2N), 2.58 (m, 2H, $NCH_2CH_2CH_2CH_3$), 1.56 (m, 2H, $NCH_2CH_2CH_2CH_3$), 1.18 (m, 2H, $NCH_2CH_2CH_2CH_3$), 0.84 (t, J = 7 Hz, 3H, $NCH_2CH_2CH_2CH_3$) ppm. ^{13}C{^{1}H} NMR ($CDCl_3$, 100.6 MHz) δ = 151.9, 147.05, 131.2, 127.8, 63.2, 58.4, 26.8, 20.1, 13.7 ppm. ^{11}B NMR ($CDCl_3$, 64.3 MHz) δ = 11 ppm. Anal. Calcd for $C_{13}H_{20}BBrN_2O_2$ (327.03): C, 47.75; H 6.16; N, 8.57. Found: C, 47.52; H 6.20; N, 8.64.

Pyridino[4,3-*c*]-1,3-dihydro-1-hydroxy-3-phenyl[2,1]oxaborole (3a). A solution of **2** (3.27 g, 10 mmol) in THF (15 mL) was added to a solution of *n*BuLi (10 M, 1.2 mL, 12 mmol) in the mixture of THF/Et_2O (1:1, 30 mL) at –85 °C. The resulting yellow slurry was stirred for 15 min, and the reaction mixture was treated with a solution of benzaldehyde (1.5 g, 14 mmol) in Et_2O (10 mL). The temperature was kept below –85 °C during the addition. The mixture was stirred for 20 min, and then it was warmed to –35 °C, followed by hydrolysis with H_2SO_4 (1.5 M aq, 9 mL, final pH = 3-4). The precipitation of a white solid was observed. Solvents were evaporated under reduced pressure and a solid residue was filtered, washed with water (5 mL) and Et_2O (5 mL). Drying in vacuo afforded the title compound (1.9 g, 81%) as a white powder, m.p. 160-200 °C (dec). Yield: 1.4 g (34%). ^{1}H NMR (DMSO-d_6, 400 MHz) δ = 9.75 (s, 1H, BOH), 8.53 (d, J = 4 Hz, 1H, Py), 8.46 (s, 1H, Py), 7.66 (d, J = 4 Hz, 1H, Py), 7.33-7.26 (m, 5H, Ph), 6.31 (s, 1H, CHOB) ppm. ^{13}C{^{1}H} NMR (DMSO-d_6, 100.6 MHz) δ = 151.8, 148.0, 144.7, 140.7, 129.1, 128.5, 126.5, 125.0, 81.0 ppm. ^{11}B NMR (DMSO-d_6, 64.3 MHz) δ = 31 ppm. Anal. Calcd for $C_{12}H_{10}BNO_2{\cdot}½H_2O$ (220.04): C, 65.50; H 5.04; N, 6.36. Found: C, 65.30; H 5.13; N, 6.17.

Pyridino[4,3-*c*]-1,3-dihydro-1-hydroxy-3-(2'-methoxyphenyl)[2,1]oxaborole (3b). This compound has been prepared as described for **3a** using *n*BuLi (10 M, 2.2 mL, 20 mmol) in THF/Et_2O (1:1, 30 mL), solution of **2** (6.54 g, 20 mmol) in THF (20 mL) and 2-methoxybenzaldehyde as the electrophile (2.72 g, 20 mmol) diluted with Et_2O (10 mL). The reaction mixture was hydrolyzed with H_2SO_4 (1.5 M aq., 14 mL), then aqueous phase was separated and extracted with Et_2O (2 × 15 mL). The extracts were added to the organic phase, which was concentrated under reduced pressure. The solid residue was filtered, washed with H_2O (5 mL) and Et_2O (5 mL). Drying in vacuo gave the title compound as a white powder, m.p. 190-220 °C (dec). Yield: 4.7 g (98%). ^{1}H NMR (DMSO-d_6, 400 MHz) δ = 8.50 (d, J = 4 Hz, 1H), 8.48 (s, 1H), 7.64 (d, J = 4 Hz, 1H), 7.27–7.23 (m, 1H), 7.04 (d, J = 8 Hz, 1H), 6.99 (d, J = 7 Hz, 1H), 6.86 (t, J = 7 Hz, 1H), 6.53 (s, 1H, CHOB), 3.82 (s, 3H, OCH_3) ppm. ^{13}C{^{1}H} NMR (DMSO-d_6, 100.6 MHz) δ = 156.7, 152.0, 147.8, 144.0, 139.9, 129.7, 128.6, 126.3, 125.1, 120.9, 111.8, 76.3, 55.9 ppm. ^{11}B NMR (DMSO-d_6, 96.3 MHz) δ = 33.0 ppm. ^{11}B NMR (D_2O/MeOH, 64.3 MHz) δ = 9.0 ppm. Anal. Calcd for $C_{13}H_{12}BNO_3$ (241.05): C, 64.77; H 5.02; N, 5.81. Found: C, 64.40; H 4.93; N, 5.64.

Pyridino[4,3-*c*]-1,3-dihydro-1-hydroxy-3-mesityl[2,1]oxaborole (3c). A solution of 2 (3.27 g, 10 mmol) in THF (15 mL) was added to a solution of *n*BuLi (10 M, 1.2 mL, 12 mmol) in the mixture of THF/Et_2O (1:1, 30 mL) at –85 °C. The resulting yellow slurry was stirred for 15 min, and the reaction mixture was treated with a mesitaldehyde[38] (2.1 g, 14 mmol) diluted with Et_2O (10 mL). The temperature was kept below –85°C. After addition, a mixture was stirred for 20 min, and then it was warmed to –35°C, followed by hydrolysis with 1.5 M aq. H_2SO_4 (9 mL, pH = 3-4). The precipitation of white solid was observed. Solvents were evaporated under reduced pressure and solid residue was filtered, washed with water (5 mL) and Et_2O (5 mL). Finally, the product was stirred with acetone (5 mL) for 30 min at 50 °C, then cooled and filtred. Drying in vacuo at 40 °C for 2 hr afforded the title compound as a white powder, m.p. 185-195 °C (dec). Yield: 1.9 g (81%). ^{1}H NMR (DMSO-d_6, 400 MHz) δ = 9.65 (br, 1H, BOH), 8.56 (d, J = 4 Hz, 1H, Py), 8.26 (s, 1H, Py), 7.70 (d, J = 4 Hz, 1H, Py), 6.91 (br, 1H, Mes), 6.65 (br, 1H, Mes), 6.61 (s, 1H, CHOB), 2.49 (br, 3H, *ortho*-Me), 2.16 (s, 3H, *para*-Me), 1.56 (br, 3H, *ortho*-Me) ppm. ^{13}C{^{1}H} NMR (DMSO-d_6, 100.6 MHz) δ = 151.2, 147.8, 143.5, 141.0 (br, C_B), 137.6, 137.1, 132.1, 131.2 (br, *C*Me), 129.7 (br, *C*Me), 124.9, 78.3, 20.87 (br, *ortho*-Me), 20.83, 20.1 (br, *ortho*-Me) ppm. ^{11}B NMR (DMSO-d_6, 96.3 MHz) δ = 34.0 ppm. Anal. Calcd for $C_{15}H_{15}NO_2$ (253.10): C, 71.18; H, 6.37; N, 5.53. Found: C, 70.97; H, 6.24; N, 5.45.

Pyridino[4,3-*c*]-1,3-dihydro-1-hydroxy-3,3-diphenyl[3,2,1]siloxaborole (4). This compound has been prepared as described for **3a** using *n*BuLi (10 M, 1.2 mL, 12 mmol) in THF/Et_2O (1:1, 20 mL), a solution of **2** (3.27 g, 10 mmol) in THF (15 mL) and chlorodiphenylsilane as the electrophile (2.84 g, 13 mmol) diluted with THF (5 mL). The reaction mixture was hydrolyzed with 1.5 M aqueous H_2SO_4 to reach the pH = 4-5, while the precipitation of a white solid was observed. Solvents were evaporated under reduced pressure and the remaining slurry was filtered, washed with water (20 mL) and acetone (2 × 5 mL). Finally, the product was stirred with acetone (5 mL) for 30 min at 50 °C, then cooled and filtered. Drying in vacuo at 40 °C for 2 hr afforded the title compound as a white powder, m.p. 230-250 °C (dec). Yield: 2.8 g (92%). ^{1}H NMR (DMSO-d_6+TfOD, 400 MHz) δ = 9.07 (br, BOH), 8.64 (br, 1H, Py), 8.28 (br, 1H, Py), 7.64 (br, 1H, Py), 7.45-7.39 (m, 10H, Ph) ppm. ^{11}B NMR (DMSO-d_6+TfOD, 96.3 MHz) δ = 20.0 ppm. Anal. Calcd for $C_{17}H_{14}BNO_2Si{\cdot}½H_2O$ (312.20): C, 65.40; H 4.84; N, 4.49. Found: C, 65.68; H 4.96; N, 4.82.

Pyridino[4,3-*c*]-1,3-dihydro-1-hydroxy-3-(2'-methoxyphenyl)[2,1]oxaborole hydrochloride ([3b-H]Cl). A sample of **3b** (0.48 g, 2 mmol) was dissolved in 1 M aq. HCl (2.1 mL, 2.1 mmol). The resulting solution was evaporated to dryness to leave a white solid, which was dried in vacuo at 40 °C for 2 hr. Yield 0.50 g (90%). ^{1}H NMR (DMSO-d_6, 300 MHz) δ = 8.78 (br, 1H, Py), 8.67 (br, 1H, Py), 8.24 (d, J = 5 Hz, 1H, Py), 7.33–7.30 (m, 1H, Ph), 7.24 (d, J = 7 Hz, 1H, Ph), 7.08 (d, J = 8 Hz, 1H, Ph), 6.93 (t, J = 7 Hz, 1H, Ph), 6.60 (s, 1H, CHOB), 3.80 (s, 3H, OMe) ppm. ^{13}C{^{1}H} NMR (DMSO-d_6, 75 MHz) δ = 156.7, 153.0, 140.7, 136.6, 130.2, 128.3, 128.0, 127.5, 121.0, 112.0, 75.9, 56.0 ppm. Anal. Calcd for $C_{13}H_{13}BNO_3Cl{\cdot}2H_2O$ (313.54): C, 49.80; H 5.46; N, 3.45. Found: C, 49.57; H 5.42; N, 3.34.

***N*-Methylpyridinium[4,3-*c*]-1,3-dihydro-1-hydroxy-3-(2'-methoxyphenyl)[2,1]oxaborole methylsulfate ([3b-Me][MeOSO$_3$]).** A mixture of **3b** (0.48 g, 2 mmol) and dimethyl sulfate (0.63 g, 5 mmol) was refluxed in acetonitrile (10 mL) for 1 hr. The resulting solution was concentrated and the residue was dissolved in water (5 mL). The solution was extracted with Et_2O to remove an excess of Me_2SO_4 and then it was evaporated to leave a white solid, which was dried in vacuo at 40 °C for 2 hr. Yield 0.45 g (62%). ^{1}H NMR (acetone-d_6, 400 MHz) δ = 8.85 (d, J = 6 Hz, 1H, Py), 8.79 (s, 1H, Py), 8.31 (d, J = 6 Hz, 1H, Py), 7.31 (m, 2H, Ph), 7.02 (d, J = 8 Hz, 1H), 6.92 (d, J = 8 Hz, 1H), 6.66 (s, 1H), 4.45 (s, 3H, MePy$^+$), 3.81 (s, 3H, OMe), 3.53 (s, 3H, $MeOSO_3$) ppm. ^{13}C{^{1}H} NMR (acetone-d_6, 100.6 MHz) δ = 156.6, 153.9, 143.3, 139.7, 130.1, 129.0, 127.1, 120.7, 111.4, 75.4, 55.2, 53.9, 48.3 ppm. According to the ^{1}H NMR analysis, the product contains some impurities which could not be removed - presumably due to their ionic nature (they may result from a cleavage of the B-C bond). Anal. Calcd for $C_{15}H_{18}BNO_7S{\cdot}1.5H_2O$ (394.21): C, 45.70; H 5.37; N, 3.55. Found: C, 45.48; H 5.31; N, 3.28.

α-(2'-Methoxyphenyl)-2-fluoro-4-iodopyridine-3-methanol (5a). A solution of 2-fluoro-3-iodopyridine[19] (4.46 g, 0.02 mol) in THF (10 mL) was added to a solution of LDA freshly prepared from diisopropylamine (2.1 g, 0.021 mol) and *n*BuLi (10 M; 2.1 mL, 0.021 mol) in THF (40 mL) at 80 °C. The lithiate was stirred for 20 min at –85 °C followed by a dropwise addition of 2-methoxybenzaldehyde (3.0 g, 0.022 mol) in Et_2O (30 mL). The mixture was stirred for 30 min at –70 °C and then it was quenched with water. Solvents were evaporated under reduced pressure to give a crude solid product which was washed with water and Et_2O (30 mL) at 5 °C. Drying in vacuo gave the title compound, m.p. 160-162 °C. Yield 5.1 g (71%). ^{1}H NMR (DMSO-d_6, 300 MHz) δ = 7.82 (dd, J = 5, 2 Hz, 1H, Py), 7.75–7.70 (m, 1H, Ph), 7.71 (dd, J = 5, 1 Hz, 1H, Py), 7.24 (ddd, J = 8, 7, 2 Hz, 1H), 7.00 (td, J = 7, 1 Hz, 1H, Ph), 6.88 (dd, J = 8, 1 Hz, 1H, Ph), 6.13 (d, J = 5 Hz, 1H, C*H*OH), 6.10 (d, J = 5 Hz, 1H, CHO*H*), 3.62 (s, 3H, OMe) ppm. ^{13}C{^{1}H} NMR (DMSO-d_6, 75.6 MHz) δ = 160.1 (d, $^1J_{CF}$ = 237 Hz), 156.1, 146.4 (d, $^2J_{CF}$ = 21 Hz), 133.4 (d, $^3J_{CF}$ = 6 Hz), 130.8, 129.1, 128.5, 127.5 (d, $^4J_{CF}$ = 5 Hz), 120.2, 115.9 (d, $^3J_{CF}$ = 6 Hz), 110.8, 71.9 (d, $^3J_{CF}$ = 5 Hz), 55.4 ppm. Anal. Calcd for $C_{13}H_{11}FINO_2$ (359.13): C, 43.48; H 3.09; N, 3.90. Found: C, 43.80; H 3.49; N, 4.04.

2-Fluoropyridino[4,3-*c*]-1,3-dihydro-1-hydroxy-3-(2'-methoxyphenyl)[2,1]oxaborole (5b). A solution of **5a** (3.6 g, 10 mmol) in THF (30 mL) was treated with NaH (60wt% dispersion in mineral oil, 0.5 g, 12.5 mmol) at 0 °C. When the evolution of H_2 ceased, the resulting suspension was cooled to –80 °C and *t*BuLi (1.7 M in pentane, 13 mL, 22 mmol) was added dropwise. The resulting red solution was stirred for 30 min at –78 °C and then $B(OMe)_3$ (2.3 g, 22 mmol) was added dropwise. The resulting mixture was stirred for 1 h at at –78 °C and then it was hydrolyzed with 2 M aqueous H_2SO_4 to reach the final pH = 4. The water phase was extracted with Et_2O (20 mL). The combined organic phase was concentrated under reduced pressure. The residue was filtered, washed with water (2 × 5 mL) and CH_2Cl_2 (2 × 5 mL) and dried in vacuo to give the title compound. The product was obtained as a white powder, m.p. 174-176 °C. Yield 1.9 g (73%). ^{1}H NMR (acetone-d_6, 300 MHz) δ = 8.74 (br, 1H, BOH), 8.25 (ddd, J = 5, 2, 1 Hz, 1H, Py), 7.67 (dd, J = 5, 4 Hz, 1H, Py), 7.34 (ddd, J = 8, 7, 2 Hz, 1H, Ph), 7.06 (dd, J = 8, 1 Hz, 1H, Ph), 7.00 (dd, J = 8, 2 Hz, 1H, Ph), 6.94–6.90 (m, 1H, Ph), 6.67 (s, 1H, CHOB), 3.82 (s, 3H, OMe) ppm. ^{13}C{^{1}H} NMR (acetone-d_6, 75.6 MHz) δ = 158.0 (d, $^1J_{CF}$ = 241 Hz), 157.8, 146.6 (d, $^3J_{CF}$ = 16 Hz), 137.1 (d, $^2J_{CF}$ = 39 Hz), 130.0, 128.0, 126.1, 122.6 (d, $^4J_{CF}$ = 7 Hz), 120.5, 111.5, 75.6 (d, $^3J_{CF}$ = 8 Hz), 55.1 ppm. ^{11}B NMR (DMSO-d_6, 96.3 MHz) δ = 33.0 ppm. ^{11}B NMR (MeOH/D_2O, 96.3 MHz) δ = 27.5 ppm. ^{19}F NMR (acetone-d_6, 282 MHz) δ = -73.47 ppm. Anal. Calcd for $C_{13}H_{11}BFNO_3$ (259.04): C, 60.28; H 4.28; N, 5.41. Found: C, 60.09; H 4.47; N, 5.42.

Thermal analyses.

DSC. Differential scanning calorimetric analysis was conducted by differential scanning calorimetry (DSC) (Model DSC 1, Mettler-Toledo) under the flow of nitrogen atmosphere. The calibration of the instrument was performed using the phase-transition temperature and phase-transition enthalpy of indium as reference material. The samples of 2-5 mg were prepared in a covered 40-μL aluminum crucible with a hole in the lid to allow venting. An empty crucible was used as a reference. The heating rate of 5 K/min from 25 °C to 300 °C in the first cycle and from 25 °C to 500 °C in the second.

TGA/DSC. Thermogravimetric analysis and simultaneous DSC analysis were performed on TGA/DSC1 (Mettler-Toledo) system under continuous flow of argon at the heating rate of 5 K/min from 30 °C to 400 °C. The samples of 5-15 mg were prepared in a covered ceramic crucibles. An empty crucible was used as a reference. α-Al_2O_3 was used for instrument calibration.

Crystallization, structural measurement and refinement details.

The single crystals of **3c** and **5b** were measured at 100 K on a SuperNova diffractometer equipped with an Atlas detector (Cu-K_α radiation, λ = 1.54184 Å). Data reduction and analysis were carried out with the *CrysAlisPro* program.[39] All structures were solved by direct methods using *SHELXS-97* and refined using *SHELXL-2013*.[40] All non-hydrogen atoms were refined anisotropically. Crystallographic Information Files (CIFs) have been deposited with the Cambridge Crystallographic Data Centre as supplementary publications no. 1406327 (**3c**) and 1406328 (**5b**).

Crystal data for **3c**: $C_{15}H_{16}BNO_2$, M_r = 253.10 a.u.; T = 100 (1) K; orthorhombic; *Pbca*; a = 12.928 (1) Å, b = 10.000 (1) Å, c = 20.181 (1) Å, V = 2609.1 (1) Å^3; d_{calc} = 1.289 g·cm^{-3}; μ = 0.67 mm^{-1}; Z = 8; F(000) = 1072; number of collected / unique reflection (R_{int} = 3.0%) = 13550 / 2055, R[F] / wR[F] (I ≥ 3σ(I)) = 4.7% / 13.5%, $\Delta\varrho_{res}^{(min/max)}$ = −0.35 / +0.43 e·Å^{-3}.

Crystal data for **5b**: $C_{13}H_{11}BFNO_3$, M_r = 259.04 a.u.; T = 100 (1) K; monoclinic; $P2_1/n$; a = 11.002 (1) Å, b = 7.962 (1) Å, c = 15.056 (1) Å, β = 110.38 (1) °; V = 1236.4 (1) Å^3; d_{calc} = 1.392 g·cm^{-3}; μ = 0.91 mm^{-1}; Z = 4; F(000) = 536; number of collected / unique reflection (R_{int} = 2.0%) = 8856 / 2568, R[F] / wR[F] (I ≥ 3σ(I)) = 4.0 % / 10.4%, $\Delta\varrho_{res}^{(min/max)}$ = −0.23 / +0.25 e·Å^{-3}.

Computational methods.

Single-molecule computation with *GAUSSIAN*. All geometry optimizations and frequency calculations were carried out with *Gaussian09* suite of programs[41] and M06-2X method was applied[31] using 6-31G(d,p)[32] basis sets. The minima were confirmed by vibrational frequency calculations within the harmonic

approximation. In optimization processes no symmetry constraints were applied. Starting geometries of corresponding molecular and dimeric entities were taken directly from the crystal structures or generated in *GausView* based on crystal structure geometries of related species. In the case of **5b'** the structure of a coordination dimer was unstable, therefore the N–B bond was constrained prior optimization to the value found in **3c** ($d_{N–B}$ = 1.678 Å). The energies of hydrogen-bonded dimers as well as N–B bond energies were calculated using supermolecular method including Basis Set Superposition Error (BSSE).

Topological analyses. In order to provide a deeper examination into the bonding relations within the studied structures, the topological analyses of the calculated electron densities (M06-2X/6-31G(d,p)) of molecules **3c'** and **5b'** with their optimised geometries was prepared and compared it with the results for pyridine. Additional analyses was performed for N–B adduct **5b'**. Topological analyses of charge density was accomplished in terms of QTAIM approach[33] and was carried out using AIM2000.[42] In the framework of this approach critical points (CPs) together with the bond paths (BPs) were found as well as charge concentrations (CCs).

Acknowledgment

This work was supported by the National Science Centre (Narodowe Centrum Nauki, Grant No. DEC-2011/03/B/ST5/02755). Theoretical calculations were done at the Interdisciplinary Centre of Mathematical and Computational Modelling in Warsaw (grant no. G33-14).

References

1. D. G. Hall, *Boronic Acids*, 2nd ed., Wiley-VCH, Weinheim, Germany, 2011.

2. (*a*) A. Adamczyk-Woźniak, M. K. Cyrański, A. Żubrowska and A. Sporzyński, *J. Organomet. Chem.,* 2009, **694**, 3533-3541; (*b*) J. Zhang, M. Y. Zhu, Y. N. Lin and H. C. Zhou, *Sci. China. Chem*., 2013, **56**, 1372-1381; (*c*) C. T. Liu, J. W. Tomsho and S. J. Benkovic, *Bioorg. Med. Chem.,* 2014, **22**, 4462-4473; (*d*) A. Adamczyk-Woźniak, K. M. Borys and A. Sporzyński, *Chem. Rev.,* 2015, DOI:10.1021/cr500642d.

3. J. W. Tomsho, A. Pal, D. G. Hall and S. J. Benkovic, *ACS Med. Chem. Lett.,* 2012, **3**, 48-52.

4. For selected applications, see: (*a*) S. J. Benkovic, S. J. Baker, M. R. K. Alley, Y. H. Woo, Y. K. Zhang, T. Akama, W. Mao; J. Baboval, P. T. R. Rajagopalan, M. Wall, L. S. Kahng, A. Tavassoli and L. Shapiro, *J. Med. Chem.,* 2005, **48**, 7468-7476; (*b*) Z. T. Qiao, Q. Wang, F. L. Zhang, Z. L. Wang, T. Bowling, B. Nare, R. T. Jacobs, J. Zhang, D. Z. Ding, Y. G. Liu and H. C. Zhou, *J. Med. Chem.,* 2012, **55**, 3553-3557; (*c*) M. P. Anthony, J. N. Burrows, S. Duparc, J. J. Moehrle and T. N. Wells, *Malar. J.,* 2012, **11**, 316-341.

5. (*a*) F. L. Rock, W. Mao, A. Yaremchuk, M. Tukalo, T. Crepin, H. C. Zhou, Y. K. Zhang, V. Hernandez, T. Akama, S. J. Baker, J. J. Plattner, J. J.; L. Shapiro, S. A. Martinis, S. J. Benkovic, S. Cusack and M. R. K. Alley, *Science,* 2007, **316**, 1759-1761; (*b*) T. Akama, S. J. Baker, Y. -K. Zhang, V. Hernandez, H. Zhou, V. Sanders, Y. Freund, R. Kimura, K. R. Maples and J. Plattner, *Bioorg. Med. Chem. Lett.,* 2009, **19**, 2129-2132; (*c*) E. Seiradake, W. Mao, V. Hernandez, S. J. Baker, J. J. Plattner, M. R. K. Alley and S. Cusack, *J. Mol. Biol.,* 2009, **390**, 196-207.

6. Anacor Pharmaceuticals. FDA Approves Anacor Pharmaceuticals' KERYDINTM (Tavaborole) Topical Solution, 5% for the Treatment of Onychomycosis of the Toenails. Press release, July 8, 2014; http://www.anacor.com/.

7. (*a*) M. Dowlut and D. G. Hall, *J. Am. Chem. Soc.*, 2006, **128**, 4226-4227; (*b*) M. Bérubé, M. Dowlut and D. G. Hall, *J. Org. Chem.,* 2008, **73**, 6471-6471.

8. A. Brzozowska, P. Ćwik, K. Durka, T. Kliś, A. E. Laudy, S. Luliński, J. Serwatowski, S. Tyski, M. Urban and W. Wróblewski, *Organometallics*, 2015, **34**, 2924−2932.

9. For the definition and use of the term „*tecton*" in crystal engineering, see: (*a*) M. Simard, D. Su and J. D. Wuest, *J. Am. Chem. Soc.*, 1991, **113**, 4696-4698; (*b*) M. W. Hosseini *CrystEngComm*, 2004, **6**, 318–322; (*c*) M. W. Hosseini, *Acc. Chem. Res.,* 2005, **38**, 313-323.

10. (*a*) J.-H. Fournier, T. Maris, J. D. Wuest, W. Guo and E. Galoppini, *J. Am. Chem. Soc.,* 2003, **125**, 1002–1006; (*b*) P. Rodríguez-Cuamatzi, G. Vargas-Díaz and H. Höpfl, *Angew. Chem. Int. Ed.,* 2004, **43**, 3041−3044; (*c*) P. Rodríguez-Cuamatzi, R. Luna-García, A. Torres-Huerta, M. I. Bernal-Uruchurtu, V. Barba and H. Höpfl, *Cryst. Growth Des.,* 2009, **9**, 1575–1583; (*d*) K. Durka, K. N. Jarzembska, R. Kamiński, S. Luliński, J. Serwatowski and K. Woźniak, *Cryst. Growth Des.,* 2012, **12**, 3720–3734; (*e*) K. Durka, K. N. Jarzembska, R. Kamiński, S. Luliński, J. Serwatowski and K. Woźniak, *Cryst. Growth Des.,* 2013, **13**, 4181–4185.

11. A. L. Korich and P. M. Iovine, *Dalton Trans.,* 2010, **39**, 1423–1431.

12. (*a*) H. M. El-Kaderi, J. R. Hunt, J. L. Mendoza-Cortés, A. P. Côté , R. E. Taylor, M. O'Keeffe and O. M. Yaghi, *Science*, 2007, **316**, 268–272; (*b*) H. Furukawa and O. M. Yaghi, *J. Am. Chem. Soc.,* 2009, **131**, 8875-8883; (*c*) S.-Y. Ding and W. Wang, *Chem. Soc. Rev.,* 2013, **42**, 548-568.

13. (*a*) N. Christinat, R. Scopelliti and K. Severin, *Chem. Commun.,* 2004, 1158-1159; (*b*) N. Christinat, R. Scopelliti and K. Severin *J. Org. Chem.,* 2007, **72**, 2192–2200; (*c*) K. Severin, *Dalton Trans.,* 2009, 5254-5264; (*d*) E. Sheepwash, V. Krampl, R. Scopelliti, O. Sereda, A. Neels and K. Severin, *Angew. Chem. Int. Ed.,* 2011, **50**, 3034-3037; (*e*) B. Icli, E. Sheepwash, T. Riis-Johannessen, K. Schenk, Y. Filinchuk, R. Scopelliti and K. Severin, *Chem. Sci.*, 2011, **2**, 1719-1721; (*f*) B. Icli, E. Solari, B. Kilbas, R. Scopelliti and K. Severin, *Chem. Eur. J.,* 2012, **18**, 14867-14874; (*g*) E. Sheepwash, N. Luisier, M. R. Krause, S. Noe, S. Kubik and K. Severin, *Chem. Commun.,* 2012, **48**, 7808-7810; (*h*) N. Luisier, K. Schenk and K. Severin, *Chem. Commun.,* 2014, **50**, 10233-10236.

14. (a) D. Salazar-Mendoza, J. Guerrero-Alvarez and H. Höpfl, *Chem. Commun.,* 2008, 6543–6545; (*b*) J. Cruz-Huerta, D. Salazar-Mendoza, J. Hernandez-Paredes, I. F. H. Ahuactzi and H. Höpfl, *Chem. Commun.,* 2012, **48**, 4241-4243; (*c*) D. Salazar-Mendoza, J. Cruz-Huerta, H. Höpfl, I. F. Hernandez-Ahuactzi and M. Sanchez, *Cryst. Growth Des.,* 2013, **13**, 2441-2454.

15. (*a*) X. Ma, Z. Yang, X. Wang, H. W. Roesky, F. Wu and H. Zhu, *Inorg. Chem*., 2011, **50**, 2010-2014; (*b*) E. Jaśkowska, I. Justyniak, M. K. Cyrański, A. Adamczyk-Woźniak, A. Sporzyński, E. Zygadło-Monikowska and W. Ziemkowska, *J. Organomet. Chem.,* 2013, **732**, 8-14.

16. (*a*) V. V. Zhdankin, P. J. Persichini, L. Zhang, S. Fix and P. Kiprof, *Tetrahedron Lett.,* 1999, **40**, 6705–6708; (*b*) A. Adamczyk-Woźniak, M. K. Cyrański, M. Jakubczyk, P. Klimentowska, A. Koll, J. Kołodziejczak, G. Pojmaj, A. Żubrowska, G. Z. Żukowska and A. Sporzyński, *J. Phys. Chem. A,* 2010, **114***,* 2324–2330; (*c*) S. Sene, D. Berthomieu, B. Donnadieu, S. Richeter, J. Vezzani, D. Granier, S. Bégu, H. Mutin, C. Gervais and D. Laurencin, *CrystEngComm,* 2014, **16**, 4999-5011.

17. (*a*) Y. Yamamoto, T. Seko and H. Nemoto, *J. Org. Chem*., 1989, **54**, 4734-4736; (*b*) G. R. Brown, D. S. Clarke, A. J. Foubister, S. Freeman, P. J. Harrison, M. C. Johnson, K. B. Mallion, J. McCormick, F. McTaggart, A. C. Reid, G. J. Smith and M. J. Taylor, *J. Med. Chem.,* 1996, **39**, 2971-2979; (*c*) P. Vedsø, P. H. Olesen and T. Hoeg-Jensen, *Synlett,* 2004, 892-894; (*d*) K. Durka, P. Kurach, S. Luliński and J. Serwatowski, *Eur. J. Org. Chem*., 2009, 4325-4332; (*e*) E. Borowska, K. Durka, S. Luliński, J. Serwatowski and K. Woźniak, *Eur. J. Org. Chem.,* 2012, 2208-2218.

18. For a review of the chemistry of lithiated organoboranes, see: T. Kliś, S. Luliński and J. Serwatowski, *Curr. Org. Chem.,* 2010, **14**, 2549-2556.

19. M. Dąbrowski, P. Kurach, S. Luliński and J. Serwatowski, *Appl. Organomet. Chem.,* 2007, **21**, 234-238.

20. (*a*) G. W. Gribble and M. G. Saulnier, *Heterocycles*, 1993, **35**, 151-169; (*b*) S. Caron and J. M. Hawkins, *J. Org. Chem.,* 1998, **63**, 2054-2055; (*c*) J. Kristensen, M. Lysén, P. Vedsø and M. Begtrup, *Org. Lett.,* 2001, **3**, 1435; (*d*) S. Luliński, J. Serwatowski and A. Zaczek, *Eur. J. Org. Chem.,* 2006, 5167-5173.

21. M. Zhu, Z. Qiu, G. P. Hiel and S. McN. Sieburth, *J. Org. Chem*., 2002, **67**, 3487-3493.

22. (*a*).D. L. Comins and J. K. Saha, *J. Org. Chem.,* 1996, **61***,* 9623-9624; (*b*) F. Guillier, F. Nivoliers, A. Cochennec, A. Godard, F. Marsais and G. Quéguiner, *Synth. Commun.*, 1996, **26**, 4421-4436; (*c*) P. Rocca, C. Cochennec, F. Marsais, L. Thomas-dit-Dumont, M. Mallet, A. Godard and G. Quéguiner, *J. Org. Chem.,* 1993, **58***,* 7832-7838.

23 F.C. Fisher and E. Havinga, *Recl. Trav. Chim. Pays Bas*, 1974, **93**, 21-24.

24. (*a*) H.C. Brown, D.H. McDaniel, *J. Am. Chem. Soc.*, 1955, **77**, 3752–3755; (*b*) C. M. Timperley, M. Bird, S. C. Heard, S. Notman, R. W. Read, J. E. H. Tattersall and S. R. Turner, *J. Fluorine Chem*., 2005, **126**, 1160-1165.

25. K. Durka, S. Luliński, J. Serwatowski and K. Woźniak, *Organometallics*, 2014, **33**, 1608-1616.

26. P. R. Westmark, S. J. Gardiner and B. D. Smith, *J. Am. Chem. Soc.,* 1996, **118**, 11093-11100.

27. (*a*) N. A. Meanwell, *J. Med. Chem*., 2011, **54**, 2529-2591; (*b*) X.-G. Hu and L. Hunter, *Beilstein J. Org. Chem.,* 2013, **9***,* 2696–2708.

28. H. Höpfl*, J. Organomet. Chem.*, 1999, **581**, 129–149.

29. F. H. Allen, *Acta Crystallogr.,* 2002, **B58**, 380-388.

30. (*a*) M. Dąbrowski, S. Luliński, J. Serwatowski and M. Szczerbińska, *Acta Crystallogr.,* 2006, **C62**, 702-704; (*b*) A. E. Thompson, A. S. Batsanov, M. R. Bryce, N. Saygili, P. R. Parry and B. Tarbit, *Tetrahedron,* 2005, **61**, 5131-5135; (*c*) K. M. Clapham, A. S. Batsanov, M. R. Bryce and B. Tarbit, *Org. Biomol. Chem.,* 2009, **7**, 2155-2161; (*d*) A. E. Smith, K. M. Clapham, A. S. Batsanov, M. R. Bryce and B. Tarbit, *Eur. J. Org. Chem.,* 2008, 1458-1463; (*e*) A. E. Thompson, G. Hughes, A. S. Batsanov, M. R. Bryce, P. R. Parry and B. Tarbit, *J. Org. Chem.,* 2005, **70**, 388-390; (*f*) P. R. Parry, C. Wang, A. S. Batsanov, M. R. Bryce and B. Tarbit, *J. Org. Chem.,* 2002, **67**, 7541-7543.

31. (*a*) Y. Zhao and D. G. Truhlar. *Theor. Chem. Account*, 2008, **120**, 215-241; (*b*) Y. Zhao and D. G. Truhlar. *J. Phys. Chem. A,* 2006, **110**, 13126-13130.

32. R. Krishnan, J. S. Binkley, R. Seeger and J. A. Pople, *J. Chem. Phys.,* 1980, **72**, 650-654.

33. (*a*) R. F. W. Bader, *Atoms in Molecules - A Quantum Theory*; Clarendon: Oxford, 1990; (*b*) R. F. W. Bader, *J. Phys. Chem. A,* 1998, **102**, 7314-7323; (*c*) R. F. W. Bader, *J. Phys. Chem. A,* 2009, **113**, 10391-10396.

34. (*a*) Yu. A. Abramov, *Acta Crystallogr.,* 1997, **A53**, 264–272; (*b*) E. Espinosa, C. Lecomte and E. Molins, *Chem. Phys. Lett.,* 1998, **300**, 745–748. (*c*) E. Espinosa, E. Molins and C. Lecomte, *Chem. Phys. Lett.,* 1998, **285**, 170–173.

35. J. P. Foster and F. Weinhold, *J. Am. Chem. Soc.,* 1980, **102**, 7211-7218.

36. For applications of this parameter, see: (*a*) M. E. Brezgunova, E. Aubert, S. Dahaoui, P. Fertey, S. Lebègue, C. Jelsch, J. A. Ángyan and E. Espinosa, *Cryst. Growth Des.,* 2012, **12**, 5373-5386; (*b*) M. E. Brezgunova, J. Lieffrig, E. Aubert, S. Dahaoui, P. Fertey, S. Lebègue, J. G. Ángyan, M. Fourmigué and E. Espinosa, *Cryst. Growth Des.,* 2013, **13**, 3283-3289.

37. (*a*) K. Durka, R. Kamiński, S. Luliński, J. Serwatowski and K. Woźniak. *Phys. Chem. Chem. Phys.*, 2010, **12**, 13126-13136; (*b*) S. Mebs, S. Grabowsky, D. Förster, R. Kickbusch, M. Hartl, L. L. Daemen, W. Morgenroth, P. Luger, B. Paulus and D. Lentz, *J. Phys. Chem. A*, 2010, **114**, 10185-10196; (*c*) U. Flierler, D. Leusser, H. Ott, G. Kehr, G. Erker, S. Grimme and D. Stalke, *Chem. Eur. J.,* 2009, **15**, 4595-4601.

38. S. Fergus, S. J. Eustace and A. F. Hegarty, *J. Org. Chem.,* 2004, **69**, 4663-4669.

39. *CrysAlis Pro Software*; Oxford Diffraction Ltd, 2010**.**

40. G. M. Sheldrick, *Acta Crystallogr. Sect. A,* 2008, **64**, 112-122.

41. M. J. Frisch, G. W. Trucks, H. B. Schlegel, G. E. Scuseria, M. A. Robb, J. R. Cheeseman, J. A. Montgomery, Jr., T. Vreven, K. N. Kudin, J. C. Burant, J. M. Millam, S. S. Iyengar, J. Tomasi, V. Barone, B. Mennucci, M. Cossi, G. Scalmani, N. Rega, G. A. Petersson, H. Nakatsuji, M. Hada, M. Ehara, K. Toyota, R. Fukuda, J. Hasegawa, M. Ishida, T. Nakajima, Y. Honda, O. Kitao, H. Nakai, M. Klene, X. Li, J. E. Knox, H. P. Hratchian, J. B. Cross, V. Bakken, C. Adamo, J. Jaramillo, R. Gomperts, R. E. Stratmann, O. Yazyev, A. J. Austin, R. Cammi, C. Pomelli, J. W. Ochterski, P. Y. Ayala, K. Morokuma, G. A. Voth, P. Salvador, J. J. Dannenberg, V. G. Zakrzewski, S. Dapprich, A. D. Daniels, M. C. Strain, O. Farkas, D. K. Malick, A. D. Rabuck, K. Raghavachari, J. B. Foresman, J. V. Ortiz, Q. Cui, A. G. Baboul, S. Clifford, J. Cioslowski, B. B. Stefanov, G. Liu, A. Liashenko, P. Piskorz, I. Komaromi, R. L. Martin, D. J. Fox, T. Keith, M. A. Al-Laham, C. Y. Peng, A. Nanayakkara, M. Challacombe, P. M. W. Gill, B. Johnson, W. Chen, M. W. Wong, C. Gonzalez and J. A. Pople, *Gaussian09*, Gaussian, Inc.: Wallingford, CT, 2010.

42. F. Biegler-König, J. Schönbohm and D. J. Bayles, *J. Comput. Chem.*, 2001, **22**, 545-559.